

# Dynamical localization and slow dynamics in quasiperiodically-driven quantum systems

Vatsana Tiwari,<sup>1</sup> Devendra Singh Bhakuni,<sup>2</sup> and Auditya Sharma<sup>1,\*</sup>

<sup>1</sup>*Department of Physics, Indian Institute of Science Education and Research, Bhopal 462066, India*

<sup>2</sup>*Department of Physics, Ben-Gurion University of the Negev, Beer-Sheva 84105, Israel*

We investigate the role of a quasiperiodically driven electric field in a disordered fermionic chain. In the clean non-interacting case, we show the emergence of dynamical localization - a phenomenon previously known to exist only for a perfect periodic drive. In contrast, in the presence of disorder, where a high-frequency periodic drive preserves Anderson localization, we show that the quasiperiodic drive destroys it and leads to slow relaxation. Considering the role of interactions, we uncover the phenomenon of *quasiperiodic driving-induced logarithmic relaxation*, where a suitably tuned drive (corresponding to dynamical localization in the clean, non-interacting limit) slows down the dynamics even when the disorder is small enough for the system to be in the ergodic phase. This is in sharp contrast to the fast relaxation seen in the undriven model, as well as the absence of thermalization (drive-induced many-body localization) exhibited by a high-frequency periodic drive.

*Introduction:* The non-equilibrium properties of a quantum system subjected to a time-dependent drive have been a topic of great interest [1–10]. Some notable phenomena associated with such driven systems include dynamical localization in kicked rotors [11–13], dynamical freezing [14–19], Floquet topological insulators [20–22], Floquet prethermalization [23–32] and time crystals [33–37], and Floquet many-body localization (MBL) [38–40]. An intriguing category of periodically driven systems involves an *electric-field drive*, which gives rise to a range of fascinating phenomena, including dynamical localization [41–45], coherent destruction of Wannier Stark localization [45–49], and super Bloch oscillations [50, 51]. Incorporating many-body interactions further opens up fascinating possibilities, such as Stark-MBL [52–61], drive-induced MBL [49, 62], and Stark time-crystals [63, 64]. A crucial question that arises is whether these characteristics persist in the absence of a perfectly periodic drive.

While an enormous body of work has been devoted to periodic drives, the exploration of the role of quasiperiodic driving has recently gained traction [65–81]. Features like prethermalization [73–75], coherence restoration [82], and quasi-time crystals [68, 70, 74, 83] are associated with such drives. Furthermore, experiments have realized dynamical phases employing quasiperiodic driving [84]. In this Letter, we explore the properties of a system driven by a *quasiperiodic electric field*. Specifically, we address the question of whether a quasiperiodic electric-field drive can give rise to dynamical localization, and if it does, what the effect of interactions and disorder on dynamical localization would be.

We address these questions by considering two discrete forms of quasiperiodic driving: Fibonacci and Thue-Morse [67, 69, 72]. For these sequences, we find that in the non-interacting limit, the phenomenon of dynamical localization occurs when the parameters of the drive are tuned appropriately. We derive the conditions under which it is realized and numerically demonstrate this using the dynamics of return probability and entanglement

Driving Protocol	$W = 0$ $U = 0$	$W \neq 0$ $U = 0$	$W \neq 0, U \neq 0$ <i>ergodic regime</i>
Undriven	Fast relaxation	Anderson localization [85]	Fast relaxation [86]
Periodic	Dynamical localization (Periodic oscillation) [41]	Anderson localization [87]	Drive-induced MBL [62]
Quasi-periodic	Dynamical localization (Periodic oscillation)	Slow relaxation $S(t) \propto t^\gamma$ , $\gamma < 1$	Drive-induced logarithmic relaxation $S(t) \propto \log t$

Table I. Schematic of the main results for the quasiperiodic drive and a comparison with existing results for the undriven and high-frequency periodic driving cases based on an analysis of the auto-correlation function and entanglement entropy. The third row contains the central findings of our work. Here,  $W, U$  refers to disorder and interaction strength, respectively.

entropy. In the presence of disorder, where the undriven system exhibits Anderson localization [85, 88], we find that the quasiperiodic drive destroys it and leads to a slow relaxation of the return probability together with a *sub-linear* growth of entanglement entropy.

In the presence of many-body interactions, dynamical localization is lost, and the system approaches the infinite-temperature state. However, the approach is notably slower when the parameters are specifically tuned at the dynamical localization point, as opposed to arbitrary parameter choices. This follows from the fact that the drive suppresses the hopping significantly at the dynamical localization point. Next, we demonstrate how the hopping suppression can be exploited to manipulate the dynamical behavior of a disordered many-body interacting system. Starting from the ergodic phase in the weak disorder limit of the undriven model, where the auto-correlation function is known to exhibit power-law decay [86], we show that a quasiperiodic electric-field drive can in fact lead to a slow logarithmic relaxation.

This is in sharp contrast to the drive-induced MBL [62] that is seen for a high-frequency periodic drive. In Table (I), the chief findings from our work are summarized alongside already established results in the literature.

*Model Hamiltonian and driving protocol:* We consider a disordered interacting one-dimensional tight-binding chain subjected to a time-dependent electric field  $\mathcal{F}(t)$ . The model Hamiltonian can be written as:

$$H = -\frac{\Delta}{4} \sum_{j=0}^{L-2} \left( c_j^\dagger c_{j+1} + h.c. \right) + \mathcal{F}(t) \sum_{j=0}^{L-1} j \left( n_j - \frac{1}{2} \right) + \sum_{j=0}^{L-1} h_j \left( n_j - \frac{1}{2} \right) + U \sum_{j=0}^{L-2} \left( n_j - \frac{1}{2} \right) \left( n_{j+1} - \frac{1}{2} \right), \quad (1)$$

where  $c_j$  and  $c_j^\dagger$  are fermionic annihilation and creation operators respectively,  $n_j$  are number operators,  $\Delta$  is the hopping strength,  $U$  is the strength of nearest-neighbor interaction, and  $h_j$  is the on-site potential taken from a uniform distribution:  $h_j \in [-W, W]$ . For the undriven case ( $\mathcal{F}(t) = 0$ ), Eqn. 1 is the standard model of MBL where a transition from an ergodic phase to an MBL phase occurs on varying the disorder strength [89–92], although the precise value of the critical disorder strength is still controversial [93, 94]. In this work, we focus only on the ergodic side of the MBL transition. For a periodic drive with time period  $T$ :  $\mathcal{F}(t+T) = \mathcal{F}(t)$ , the clean non-interacting limit ( $W = 0, U = 0$ ) exhibits dynamical localization for appropriately tuned driving amplitude and frequency [41, 42, 49], while for a randomly fluctuating field there is no dynamical localization [48]. In this work, we focus on the case where the time-dependent field is neither periodic nor random but is rather quasiperiodic in nature and contains many frequencies in the Fourier spectrum. We allow the field  $\mathcal{F}$  to oscillate between  $\pm F$  after each period  $T$  mimicking the Fibonacci and Thue-Morse sequences [67, 68, 74].

In order to describe our driving protocol, it is convenient to introduce the unitary operators  $U_{B/A} = e^{-iT H_{B/A}}$  where  $H_{A/B}$  are the Hamiltonians corresponding to the field  $\mathcal{F}(t) = \pm F$  respectively (Eq. (1)). For the Fibonacci sequence, we start from the unitary operators  $U_0 = U_A$  and  $U_1 = U_B$ , and generate the subsequent evolution according to the Fibonacci sequence [72]:

$$U_n = U_{n-2} U_{n-1}, \quad n \geq 2. \quad (2)$$

The Thue-Morse sequence (TMS), on the other hand, can be generated using the recurrence relation [74]

$$U_{n+1} = \tilde{U}_n U_n, \quad \tilde{U}_{n+1} = U_n \tilde{U}_n, \quad (3)$$

where we start with the unitary operators  $U_1 = U_B U_A$ ,  $\tilde{U}_1 = U_A U_B$ . The time evolution of an initial state can be expressed as:  $|\psi_n\rangle = U_n |\psi(0)\rangle$ .

*Dynamical localization:* We first consider the clean non-interacting limit ( $W = 0, U = 0$ ). In this case,

the Hamiltonian (1) can be written in terms of the unitary operators: [95]  $\hat{K} = \sum_{n=-\infty}^{n=\infty} |n\rangle\langle n+1|$ ,  $\hat{K}^\dagger = \sum_{n=-\infty}^{n=\infty} |n+1\rangle\langle n|$ , and  $\hat{N} = \sum_{n=-\infty}^{n=\infty} n |n\rangle\langle n|$ , as

$$\hat{H} = -\frac{\Delta}{4} \left( \hat{K} + \hat{K}^\dagger \right) + \mathcal{F}(t) \hat{N}. \quad (4)$$

These operators follow the commutation relations:  $[\hat{K}, \hat{N}] = \hat{K}$ ,  $[\hat{K}^\dagger, \hat{N}] = -\hat{K}^\dagger$ ,  $[\hat{K}, \hat{K}^\dagger] = 0$ . With this form of the Hamiltonian and the commutation relations, we can write down the effective Hamiltonian  $H_{\text{eff}}$ . For Thue-Morse driving, we work out an expression for the stroboscopic unitary operator defined at the  $m^{\text{th}}$  Thue-Morse level:  $U(N = 2^m)$ . With the aid of Eq. (3), we can express  $U$  as a product of a string of the unitary operators  $U_A$  and  $U_B$ , which using the Baker–Campbell–Hausdorff formula [96], can be written in terms of  $H_{\text{eff}}$  as [97]

$$U(N = 2^m) \equiv \exp(-i2^m T H_{\text{eff}}). \quad (5)$$

Here,  $H_{\text{eff}}$  is given by

$$H_{\text{eff}} \equiv \Delta_{\text{eff}} \left( \hat{K} + \hat{K}^\dagger \right), \quad \Delta_{\text{eff}} = -\frac{\Delta}{4} \left[ \frac{\sin(2F\pi/\omega)}{(2F\pi/\omega)} \right], \quad (6)$$

where,  $\omega = \frac{2\pi}{T}$ . Thus we see from Eq. (6) that the coefficients of  $\hat{K}$  and  $\hat{K}^\dagger$  get renormalized. When the amplitude of the drive is tuned at  $\frac{F}{\omega} = \frac{n}{2}$  ( $n \in \mathbb{Z}$ ),  $\Delta_{\text{eff}}$  vanishes and any state will return to itself after a time period  $T$ , and thus, the system remains dynamically localized. Similar results are obtained for Fibonacci driving [97].

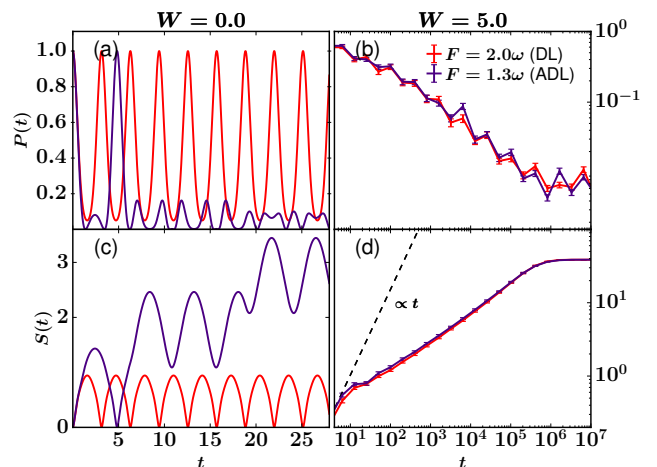


Figure 1. (a,b) Return probability  $P(t)$ , and (c,d) entanglement entropy  $S(t)$  for a Thue-Morse driven clean ( $W = 0.0$ ) and disordered ( $W = 5.0$ ) system at dynamical localization (DL) ( $F = 2.0\omega$ ) and away from it (ADL) ( $F = 1.3\omega$ ). The other parameters are  $\Delta = 4.0, \omega = 1.0, L = 200$ . We take the time discretization  $dt = 0.001$  for (a,c). The data is averaged over 100 realizations of disorder for (b,d). The black dashed line provide a guide to the ballistic growth.

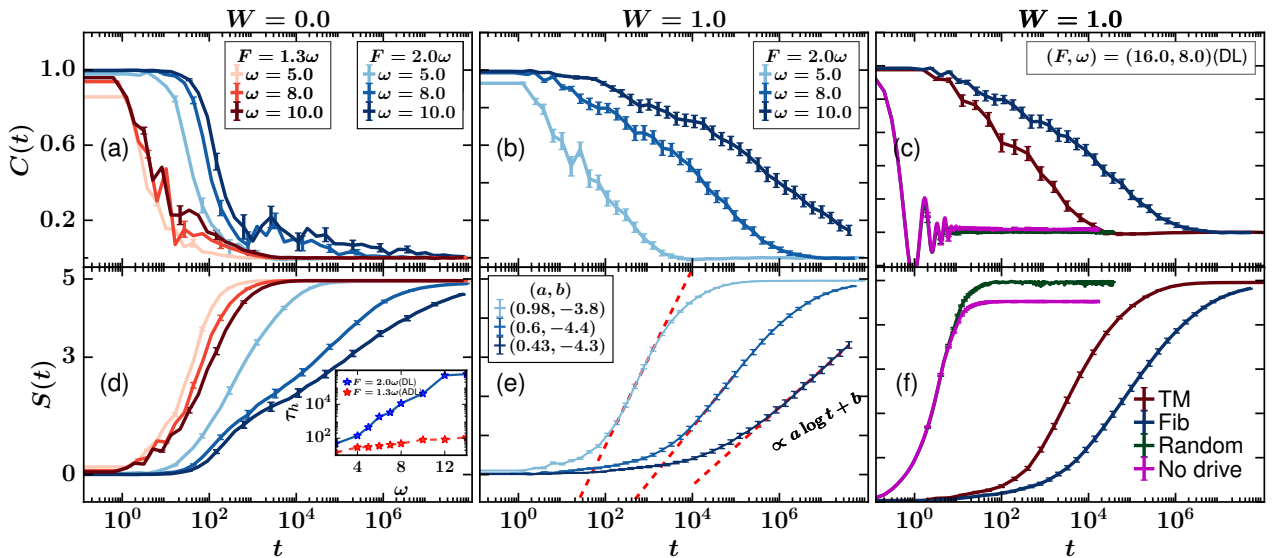


Figure 2. Dynamics of the auto-correlation function  $C(t)$  and the half chain entanglement entropy  $S(t)$  for the Fibonacci driven interacting fermionic system. (a, d): for  $W = 0.0$ . The red shades correspond to a tuning of the parameters away from dynamical localization ( $F = 1.3\omega$ , ADL), and blue shades correspond to a tuning at dynamical localization ( $F = 2.0\omega$ , DL). The inset shows the heating time  $\tau_h$  as a function of  $\omega$ . (b, e): for  $W = 1.0$ . When disorder is present, we have averaged over 100 disorder realizations. In (e), the red dashed lines are fits to the function  $a \log t + b$ . (c, f): Comparison of dynamics of differently driven and undriven interacting disordered systems. The other parameters are  $\Delta = 4.0, U = 1.0, F = 2.0\omega$ , and  $L = 16$ .

The return probability, which is a measure of the probability of finding a particle at an initially localized site  $n$  after a time  $t$  is defined as  $P(t) = |\langle \psi(0) | \psi(t) \rangle|^2$ ; in our study, we take  $n = L/2$ . The dynamics of the return probability for the Thue-Morse driven system is plotted in Fig. 1(a). For the ratio  $F/\omega = 2$ , we find that the return probability has oscillatory behavior. We have checked using stroboscopic dynamics that it periodically returns to its original value of unity even for very long times. On the other hand, tuning the ratio at  $F/\omega = 1.3$ , we see that the return probability is vanishingly small. A similar observation can be made when looking at the growth of entanglement entropy defined as [98–100]:  $S(t) = -\text{Tr}(\rho_{L/2} \ln \rho_{L/2})$ , where  $\rho_{L/2} = \text{Tr}_{1 \leq i \leq L/2} \{ |\psi(t)\rangle \langle \psi(t)| \}$  is the reduced density matrix of half the chain obtained by tracing out the other half of the chain. Starting with an initial Néel state  $|\psi(0)\rangle = \prod_{i=1}^{L/2} \hat{c}_{2i}^\dagger |0\rangle$ , we study the dynamics of the entropy in Fig. 1(c). Again, when  $F/\omega = 2$ , we find oscillatory behavior, while for  $F/\omega = 1.3$ ,  $S(t)$  starts to grow in time. These observations confirm the analytical prediction that when the ratio  $F/\omega$  is tuned properly, the system exhibits dynamical localization; else, it behaves like a nearest-neighbor chain with renormalized hopping.

*Slow dynamics in the disordered non-interacting system:* We now consider the disordered case, which leads to Anderson localization for any non-zero value of the disorder strength in the undriven model [85]. We study the stroboscopic evolution of the return probability and

the entanglement entropy for disorder strength  $W = 5.0$ . From Fig. 1(b), we see no sign of either dynamical or Anderson localization; instead, we observe that Thue-Morse driving leads to a slow decay of the return probability accompanied by a sub-linear growth of the entropy  $S(t) \propto t^\gamma$  where  $\gamma < 1$  [101]. This is in stark contrast with the effect of a high-frequency periodic drive, where Anderson localization remains stable [87, 102].

An understanding of the slow dynamics of a quasi-periodically driven system can be obtained by performing a high-frequency expansion for the first two cycles, for which the effective Hamiltonian can be written as

$$H_{\text{eff}} = \Delta_{\text{eff}} \{ \hat{K} e^{-iFT/4} + \hat{K}^\dagger e^{iFT/4} \} + D_0 + H_{\text{LRH}}, \quad (7)$$

where  $D_0$  is the static disorder term and  $H_{\text{LRH}}$  contains the longer-range hopping terms. A derivation of Eqn. 7 and the form of  $H_{\text{LRH}}$  is provided in Ref. [97]. When dealing with higher order terms and a higher level of the quasiperiodic sequence, the calculations become more complex. However, valuable information can still be extracted from  $H_{\text{eff}}$  at this level. For frequencies larger than the local bandwidth  $\Delta_\xi$  of a system of size of the order of the localization length  $\xi$ ,  $H_{\text{LRH}}$  can be neglected since it contains factors involving powers of the time period  $T$  which becomes very small. Moreover due to the renormalization  $\Delta_{\text{eff}}$ , the effective disorder increases, i.e.  $H_{\text{eff}}(J, W) \approx H(J, W/J_{\text{eff}})$  and hence a stronger localization would be expected. Thus  $H_{\text{eff}}$  obtained for two cycles suggests the stability of Anderson localization

in the presence of a high frequency drive. For a periodic drive, these two cycles repeat indefinitely; therefore, indeed this robustness of Anderson localization in the presence of high frequency periodic drive has been reported [87, 102]. For our drive protocol, however, we must incorporate higher levels of the quasiperiodic sequence. This introduces a mixture of low and high frequency components. While frequencies larger than the local bandwidth  $\omega \gg \Delta_\xi$  do not influence localization, lower frequencies  $\omega \ll \Delta_\xi$  initiate transitions between the localized states. This competition gives rise to a gradual relaxation of  $P(t)$  and a sub-linear growth of  $S(t)$ , ultimately leading to delocalization.

*Slow dynamics in the disordered interacting system:* Having discussed the emergence of dynamical localization under quasiperiodic driving, we now explore the interplay of quasiperiodic driving, many-body interactions, and disorder. We employ exact diagonalization for a system of size  $L = 16$  at half-filling and focus on the dynamics of entanglement entropy and auto-correlation function. For driven quantum systems, the entanglement entropy typically saturates to the Page value:  $S_{\text{Page}} = \frac{1}{2}(L \ln 2 - 1)$  which corresponds to the infinite temperature state [103]. The auto-correlation function is defined as [86, 104–106]

$$C(t) = 4 \langle \hat{S}_{L/2}^z(t) \hat{S}_{L/2}^z(0) \rangle, \quad (8)$$

where  $\hat{S}_i^z = \hat{n}_i - \frac{1}{2}$ . While in the localized phase, the auto-correlation function  $C(t)$  saturates to a non-zero value, in the ergodic phase, it rapidly goes to zero [68, 86].

We first start with the clean limit  $W = 0$ , and observe that dynamical localization is destroyed in the presence of many-body interactions. However, for Fibonacci driving (and also Thue-Morse [97]), the dynamics is found to be very slow if the interactions are turned on at the dynamical localization point as opposed to any arbitrary choice of the parameters. In Fig. 2(a,d), we plot the dynamics of auto-correlation  $C(t)$ , and entanglement entropy  $S(t)$  for  $\frac{F}{\omega} = 2$  (at DL) and  $\frac{F}{\omega} = 1.3$  (away from DL) and a range of driving frequencies. We average the quantities over 50 different initial product states close to the Néel state. The entanglement entropy rapidly reaches the Page value while the auto-correlation function quickly decays to zero for  $\frac{F}{\omega} = 1.3$  for all the driving frequencies considered. On the other hand, for  $\frac{F}{\omega} = 2$ ,  $C(t)$  exhibits a slow decay accompanied by a slow relaxation of  $S(t)$  to the Page value (Fig. 2(a,d)). On increasing the driving frequency, the growth further slows down, suggesting slow heating.

We next consider the disordered case with  $W = 1.0$ , which in the undriven model, lies in the ergodic region where  $C(t)$  shows fast decay [86]. We plot the auto-correlation and the entanglement entropy for Fibonacci driving in Fig. 2(b,e) for different driving frequencies and with the parameters tuned at the dynamical localization point. Although the undriven system lies in the ergodic regime, we see that the quasiperiodic drive induces loga-

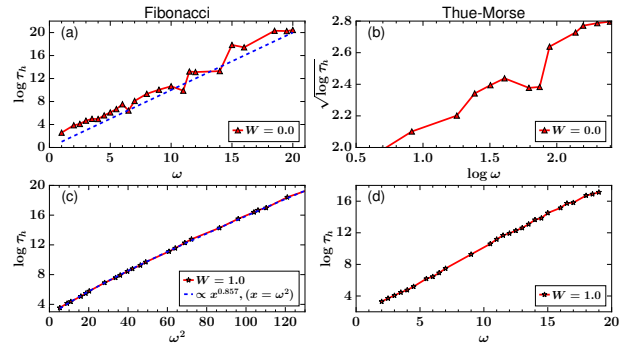


Figure 3. Heating time as a function of frequency for Fibonacci and Thue-Morse driving. (a,b)  $W = 0.0$ . (c,d)  $W = 1.0$ . The other model parameters are  $J = 1, U = 1, F = 2\omega$ .

arithmically slow relaxation of the auto-correlation and a slow growth of the entropy. Earlier work has reported a logarithmic relaxation in the MBL phase alone [68].

These findings can be understood through a high-frequency expansion analysis. Analogous to the non-interacting case, by considering the first two cycles, we get  $H_{\text{eff}}(\Delta, W, U) \approx H(\Delta_{\text{eff}}, W, U)$  [97]. This implies a suppression of hopping or, conversely, an augmented effective disorder strength  $W/\Delta_{\text{eff}}$ , driving the system towards the MBL regime [49, 62]. However, when we incorporate higher terms of the quasi-periodic sequence, low-frequency components come into play, prohibiting the possibility of MBL. Nevertheless, a competition between the low and high-frequency components emerges, leading to slow relaxation of  $C(t)$  and logarithmic growth of  $S(t)$ . The interplay between these components is also reflected in the lifetime of the slowly relaxing phase observed in the different driving protocols, as shown in Fig. 2(c, f). While a random drive with numerous low-frequency components yields fast relaxation, quasiperiodic driving results in a prolonged relaxation phase, with Fibonacci driving exhibiting even slower relaxation compared to Thue-Morse driving. This distinction can be attributed to the additional low-frequency components present in the Fourier spectrum of the Thue-Morse drive. A similar argument holds for the clean limit, where due to the hopping renormalization, we see a slow heating at dynamical localization as compared to away from it.

To investigate the impact of driving frequency on slow dynamics, we examined the heating time  $\tau_h$  defined as the time when  $S(t)$  attains half of the Page value [107], at different driving frequencies tuned at the dynamical localization point. We see that at the dynamical localization point, the heating time is several orders of magnitude greater than when the parameters are tuned away from it (Fig. 2(d) inset). Fig. 3 illustrates the relationship between  $\tau_h$  and  $\omega$  for both Fibonacci and Thue-Morse driving, considering cases with  $W = 0.0$  and  $W = 1.0$ . For  $W = 0.0$  (Fig. 3(a, b)), we observe an exponential de-

pendence of  $\tau_h$  on  $\omega$  for Fibonacci driving, whereas Thue-Morse driving follows a sub-exponential ( $\tau_h \sim e^{[\ln\omega]^2}$ ) trend consistent with the theoretical bound [24]. On the other hand, for  $W = 1.0$ , where drive induces logarithmic relaxation, an extended heating time is evident. Fibonacci driving now displays a super-exponential dependence ( $\tau_h \sim e^{\omega^\beta}$ ,  $\beta > 1$ ), while Thue-Morse driving exhibits an exponential dependence.

*Conclusions:* We investigate the dynamics of fermions in a disordered potential under the influence of a time-dependent electric field generated from Fibonacci and Thue-Morse sequences. In the absence of interactions and disorder, we demonstrate that dynamical localization can be achieved through quasiperiodic driving and identify the conditions for its realization. When disorder is introduced, the quasiperiodic drive disrupts Anderson localization but leads to a slow relaxation of observables. By introducing interactions to a system near the dynamical localization point, we show a significant suppression of heating compared to cases where parameters deviate from it. Furthermore, utilizing the concept of hopping suppression, we show a logarithmic relaxation induced by quasiperiodic driving in the ergodic regime of an interacting system. This drive-induced slow relaxation alters the dependence of heating time on the driving frequency, resulting in a super-exponential dependence for Fibonacci driving and an exponential dependence for Thue-Morse driving, contrasting the expected exponential and sub-exponential dependencies [68, 75].

We look forward to our work inspiring ways to host non-equilibrium phases of matter such as time quasicrystals [68, 74]. In general, it would be intriguing to explore the possibility of using quasiperiodic electric field drive to manipulate the properties of quantum systems in the same spirit as a periodic drive. In the future, it will be interesting to see features like coherent/incoherent destruction of Wannier-Stark localization [47, 108], super-Bloch oscillations [50, 51], and the effect of long-range interaction in such systems.

We are grateful to the High Performance Computing(HPC) facility at IISER Bhopal, where large-scale calculations in this project were run. We acknowledge QuSpin package [109, 110] for help in the numerical exact-diagonalization. V.T is grateful to DST-INSPIRE for her PhD fellowship. A.S acknowledges financial support from SERB via the grant (File Number: CRG/2019/003447), and from DST via the DST-INSPIRE Faculty Award [DST/INSPIRE/04/2014/002461]. We thank Arnab Das for helpful comments.

---

\* [auditya@iiserb.ac.in](mailto:auditya@iiserb.ac.in)

[1] M. Grifoni and P. Hänggi, Driven quantum tunneling, *Physics Reports* **304**, 229 (1998).

- [2] L. D'Alessio and M. Rigol, Long-time behavior of isolated periodically driven interacting lattice systems, *Phys. Rev. X* **4**, 041048 (2014).
- [3] A. Lazarides, A. Das, and R. Moessner, Equilibrium states of generic quantum systems subject to periodic driving, *Phys. Rev. E* **90**, 012110 (2014).
- [4] A. Lazarides, A. Das, and R. Moessner, Periodic thermodynamics of isolated quantum systems, *Phys. Rev. Lett.* **112**, 150401 (2014).
- [5] M. Bukov, L. D'Alessio, and A. Polkovnikov, Universal high-frequency behavior of periodically driven systems: from dynamical stabilization to Floquet engineering, *Advances in Physics* **64**, 139 (2015).
- [6] A. Eckardt and E. Anisimovas, High-frequency approximation for periodically driven quantum systems from a Floquet-space perspective, *New Journal of Physics* **17**, 093039 (2015).
- [7] P. Ponte, A. Chandran, Z. Papić, and D. A. Abanin, Periodically driven ergodic and many-body localized quantum systems, *Annals of Physics* **353**, 196 (2015).
- [8] J. Eisert, M. Friesdorf, and C. Gogolin, Quantum many-body systems out of equilibrium, *Nature Physics* **11**, 124 (2015).
- [9] V. Khemani, A. Lazarides, R. Moessner, and S. L. Sondhi, Phase structure of driven quantum systems, *Phys. Rev. Lett.* **116**, 250401 (2016).
- [10] W. W. Ho, T. Mori, D. A. Abanin, and E. G. D. Torre, Quantum and classical Floquet prethermalization [10.48550/arxiv.2212.00041](https://arxiv.org/abs/2212.00041) (2022).
- [11] G. Casati and J. Ford, Stochastic behavior in classical and quantum Hamiltonian systems **93**, [10.1007/BFB0021732](https://arxiv.org/abs/10.1007/BFB0021732) (1979).
- [12] D. R. Grempel, R. E. Prange, and S. Fishman, Quantum dynamics of a nonintegrable system, *Phys. Rev. A* **29**, 1639 (1984).
- [13] G. Lemarié, J. Chabé, P. Szriftgiser, J. C. Garreau, B. Grémaud, and D. Delande, Observation of the anderson metal-insulator transition with atomic matter waves: Theory and experiment, *Phys. Rev. A* **80**, 043626 (2009).
- [14] A. Das, Exotic freezing of response in a quantum many-body system, *Phys. Rev. B* **82**, 172402 (2010).
- [15] A. Roy and A. Das, Fate of dynamical many-body localization in the presence of disorder, *Phys. Rev. B* **91**, 121106 (2015).
- [16] A. Haldar and A. Das, Dynamical many-body localization and delocalization in periodically driven closed quantum systems, *Annalen der Physik* **529**, 1600333 (2017).
- [17] A. Haldar, R. Moessner, and A. Das, Onset of Floquet thermalization, *Phys. Rev. B* **97**, 245122 (2018).
- [18] A. Haldar, D. Sen, R. Moessner, and A. Das, Dynamical Freezing and Scar Points in Strongly Driven Floquet Matter: Resonance vs Emergent Conservation Laws, *Phys. Rev. X* **11**, 021008 (2021).
- [19] A. Haldar and A. Das, Statistical mechanics of Floquet quantum matter: exact and emergent conservation laws, *Journal of Physics: Condensed Matter* **34**, 234001 (2022).
- [20] T. Kitagawa, E. Berg, M. Rudner, and E. Demler, Topological characterization of periodically driven quantum systems, *Phys. Rev. B* **82**, 235114 (2010).
- [21] N. H. Lindner, G. Refael, and V. Galitski, Floquet topological insulator in semiconductor quantum wells, *Nature* **431**, 362 (2003).

- ture Physics **7**, 490 (2011).
- [22] F. Nathan, D. Abanin, E. Berg, N. H. Lindner, and M. S. Rudner, Anomalous Floquet insulators, *Phys. Rev. B* **99**, 195133 (2019).
- [23] D. A. Abanin, W. De Roeck, and F. Huveneers, Exponentially slow heating in periodically driven many-body systems, *Phys. Rev. Lett.* **115**, 256803 (2015).
- [24] T. Mori, T. Kuwahara, and K. Saito, Rigorous bound on energy absorption and generic relaxation in periodically driven quantum systems, *Phys. Rev. Lett.* **116**, 120401 (2016).
- [25] D. A. Abanin, W. De Roeck, W. W. Ho, and F. Huveneers, Effective Hamiltonians, prethermalization, and slow energy absorption in periodically driven many-body systems, *Phys. Rev. B* **95**, 014112 (2017).
- [26] D. Abanin, W. De Roeck, W. W. Ho, and F. Huveneers, A rigorous theory of many-body prethermalization for periodically driven and closed quantum systems, *Communications in Mathematical Physics* **354**, 809 (2017).
- [27] S. A. Weidinger and M. Knap, Floquet prethermalization and regimes of heating in a periodically driven, interacting quantum system, *Scientific Reports* **7**, 45382 (2017).
- [28] W. Bearez, O. Janes, A. Akkiraju, A. Pillai, A. Oddo, P. Reshetikhin, E. Druga, M. McAllister, M. Elo, B. Gilbert, D. Suter, and A. Ajoy, Floquet Prethermalization with Lifetime Exceeding 90 s in a Bulk Hyperpolarized Solid, *Phys. Rev. Lett.* **127**, 170603 (2021).
- [29] P. Peng, C. Yin, X. Huang, C. Ramanathan, and P. Cappellaro, Floquet prethermalization in dipolar spin chains, *Nature Physics* **17**, 444 (2021).
- [30] C. Fleckenstein and M. Bukov, Prethermalization and thermalization in periodically driven many-body systems away from the high-frequency limit, *Phys. Rev. B* **103**, L140302 (2021).
- [31] C. Fleckenstein and M. Bukov, Thermalization and prethermalization in periodically kicked quantum spin chains, *Phys. Rev. B* **103**, 144307 (2021).
- [32] A. Morningstar, M. Hauru, J. Beall, M. Ganahl, A. G. Lewis, V. Khemani, and G. Vidal, Simulation of Quantum Many-Body Dynamics with Tensor Processing Units: Floquet Prethermalization, *PRX Quantum* **3**, 020331 (2022).
- [33] D. V. Else, B. Bauer, and C. Nayak, Floquet Time Crystals, *Phys. Rev. Lett.* **117**, 090402 (2016).
- [34] N. Y. Yao, A. C. Potter, I.-D. Potirniche, and A. Vishwanath, Discrete time crystals: Rigidity, criticality, and realizations, *Phys. Rev. Lett.* **118**, 030401 (2017).
- [35] J. Zhang, P. W. Hess, A. Kyprianidis, P. Becker, A. Lee, J. Smith, G. Pagano, I.-D. Potirniche, A. C. Potter, A. Vishwanath, N. Y. Yao, and C. Monroe, Observation of a discrete time crystal, *Nature* **543**, 217 (2017).
- [36] B. Huang, Y.-H. Wu, and W. V. Liu, Clean Floquet Time Crystals: Models and Realizations in Cold Atoms, *Phys. Rev. Lett.* **120**, 110603 (2018).
- [37] V. Khemani, R. Moessner, and S. L. Sondhi, A brief history of time crystals [10.48550/arxiv.1910.10745](https://arxiv.org/abs/10.48550/arxiv.1910.10745) (2019).
- [38] A. Lazarides, A. Das, and R. Moessner, Fate of many-body localization under periodic driving, *Phys. Rev. Lett.* **115**, 030402 (2015).
- [39] P. Ponte, Z. Papić, F. Huveneers, and D. A. Abanin, Many-body localization in periodically driven systems, *Phys. Rev. Lett.* **114**, 140401 (2015).
- [40] D. A. Abanin, W. De Roeck, and F. Huveneers, Theory of many-body localization in periodically driven systems, *Annals of Physics* **372**, 1 (2016).
- [41] D. H. Dunlap and V. M. Kenkre, Dynamic localization of a charged particle moving under the influence of an electric field, *Phys. Rev. B* **34**, 3625 (1986).
- [42] D. Dunlap and V. Kenkre, Dynamic localization of a particle in an electric field viewed in momentum space: Connection with Bloch oscillations, *Physics Letters A* **127**, 438 (1988).
- [43] H. Lignier, C. Sias, D. Ciampini, Y. Singh, A. Zenesini, O. Morsch, and E. Arimondo, Dynamical control of matter-wave tunneling in periodic potentials, *Phys. Rev. Lett.* **99**, 220403 (2007).
- [44] A. Eckardt, M. Holthaus, H. Lignier, A. Zenesini, D. Ciampini, O. Morsch, and E. Arimondo, Exploring dynamic localization with a bose-einstein condensate, *Phys. Rev. A* **79**, 013611 (2009).
- [45] D. S. Bhakuni and A. Sharma, Characteristic length scales from entanglement dynamics in electric-field-driven tight-binding chains, *Phys. Rev. B* **98**, 045408 (2018).
- [46] M. Holthaus, G. H. Ristow, and D. W. Hone, Random Lattices in Combined a.c. and d.c. Electric Fields: Anderson vs. Wannier-Stark Localization, *Europhysics Letters (EPL)* **32**, 241 (1995).
- [47] M. Holthaus, G. H. Ristow, and D. W. Hone, ac-field-controlled anderson localization in disordered semiconductor superlattices, *Phys. Rev. Lett.* **75**, 3914 (1995).
- [48] V. Tiwari, D. S. Bhakuni, and A. Sharma, Noise-induced dynamical localization and delocalization, *Phys. Rev. B* **105**, 165114 (2022).
- [49] D. S. Bhakuni, R. Nehra, and A. Sharma, Drive-induced many-body localization and coherent destruction of Stark many-body localization, *Phys. Rev. B* **102**, 024201 (2020).
- [50] K. Kudo and T. S. Monteiro, Theoretical analysis of super-Bloch oscillations, *Phys. Rev. A* **83**, 053627 (2011).
- [51] S. Longhi and G. Della Valle, Correlated super-Bloch oscillations, *Phys. Rev. B* **86**, 075143 (2012).
- [52] M. Schulz, C. A. Hooley, R. Moessner, and F. Pollmann, Stark Many-Body Localization, *Phys. Rev. Lett.* **122**, 040606 (2019).
- [53] D. S. Bhakuni and A. Sharma, Entanglement and thermodynamic entropy in a clean many-body-localized system, *Journal of Physics: Condensed Matter* **32**, 255603 (2020).
- [54] W. Morong, F. Liu, P. Becker, K. S. Collins, L. Feng, A. Kyprianidis, G. Pagano, T. You, A. V. Gorshkov, and C. Monroe, Observation of stark many-body localization without disorder, *Nature* **599**, 393 (2021).
- [55] Q. Guo, C. Cheng, H. Li, S. Xu, P. Zhang, Z. Wang, C. Song, W. Liu, W. Ren, H. Dong, R. Mondaini, and H. Wang, Stark many-body localization on a superconducting quantum processor, *Phys. Rev. Lett.* **127**, 240502 (2021).
- [56] S. R. Taylor, M. Schulz, F. Pollmann, and R. Moessner, Experimental probes of stark many-body localization, *Phys. Rev. B* **102**, 054206 (2020).
- [57] E. van Nieuwenburg, Y. Baum, and G. Refael, From Bloch oscillations to many-body localization in clean interacting systems, *Proceedings of the National Academy of Sciences* **116**, 9269 (2019).
- [58] D. S. Bhakuni and A. Sharma, Stability of electric field

- driven many-body localization in an interacting long-range hopping model, *Phys. Rev. B* **102**, 085133 (2020).
- [59] P. Ribeiro, A. Lazarides, and M. Haque, Many-Body Quantum Dynamics of Initially Trapped Systems due to a Stark Potential: Thermalization versus Bloch Oscillations, *Phys. Rev. Lett.* **124**, 110603 (2020).
- [60] E. V. H. Doggen, I. V. Gornyi, and D. G. Polyakov, Stark many-body localization: Evidence for hilbert-space shattering, *Phys. Rev. B* **103**, L100202 (2021).
- [61] G. Zisling, D. M. Kennes, and Y. Bar Lev, Transport in stark many-body localized systems, *Phys. Rev. B* **105**, L140201 (2022).
- [62] E. Bairey, G. Refael, and N. H. Lindner, Driving induced many-body localization, *Phys. Rev. B* **96**, 020201 (2017).
- [63] A. Kshetrimayum, J. Eisert, and D. M. Kennes, Stark time crystals: Symmetry breaking in space and time, *Phys. Rev. B* **102**, 195116 (2020).
- [64] S. Liu, S.-X. Zhang, C.-Y. Hsieh, S. Zhang, and H. Yao, Discrete Time Crystal Enabled by Stark Many-Body Localization, *Phys. Rev. Lett.* **130**, 120403 (2023).
- [65] G. Abal, R. Donangelo, A. Romanelli, A. C. Sicardi Schifino, and R. Siri, Dynamical localization in quasiperiodic driven systems, *Phys. Rev. E* **65**, 046236 (2002).
- [66] A. Verdeny, J. Puig, and F. Mintert, Quasi-periodically driven quantum systems, *Zeitschrift für Naturforschung A* **71**, 897 (2016).
- [67] S. Nandy, A. Sen, and D. Sen, Aperiodically driven integrable systems and their emergent steady states, *Phys. Rev. X* **7**, 031034 (2017).
- [68] P. T. Dumitrescu, R. Vasseur, and A. C. Potter, Logarithmically slow relaxation in quasiperiodically driven random spin chains, *Phys. Rev. Lett.* **120**, 070602 (2018).
- [69] S. Nandy, A. Sen, and D. Sen, Steady states of a quasiperiodically driven integrable system, *Phys. Rev. B* **98**, 245144 (2018).
- [70] K. Giergiel, A. Kuroś, and K. Sacha, Discrete time quasicrystals, *Phys. Rev. B* **99**, 220303 (2019).
- [71] S. Ray, S. Sinha, and D. Sen, Dynamics of quasiperiodically driven spin systems, *Phys. Rev. E* **100**, 052129 (2019).
- [72] S. Maity, U. Bhattacharya, A. Dutta, and D. Sen, Fibonacci steady states in a driven integrable quantum system, *Phys. Rev. B* **99**, 020306 (2019).
- [73] D. V. Else, W. W. Ho, and P. T. Dumitrescu, Long-lived interacting phases of matter protected by multiple time-translation symmetries in quasiperiodically driven systems, *Phys. Rev. X* **10**, 021032 (2020).
- [74] H. Zhao, F. Mintert, R. Moessner, and J. Knolle, Random multipolar driving: Tunably slow heating through spectral engineering, *Phys. Rev. Lett.* **126**, 040601 (2021).
- [75] T. Mori, H. Zhao, F. Mintert, J. Knolle, and R. Moessner, Rigorous bounds on the heating rate in thue-morse quasiperiodically and randomly driven quantum many-body systems, *Phys. Rev. Lett.* **127**, 050602 (2021).
- [76] H. Zhao, F. Mintert, J. Knolle, and R. Moessner, Localization persisting under aperiodic driving, *Phys. Rev. B* **105**, L220202 (2022).
- [77] D. M. Long, P. J. D. Crowley, and A. Chandran, Many-body localization with quasiperiodic driving, *Phys. Rev. B* **105**, 144204 (2022).
- [78] T. Martin, I. Martin, and K. Agarwal, Effect of quasiperiodic and random noise on many-body dynamical decoupling protocols, *Phys. Rev. B* **106**, 134306 (2022).
- [79] H. Zhao, J. Knolle, R. Moessner, and F. Mintert, Suppression of interband heating for random driving, *Phys. Rev. Lett.* **129**, 120605 (2022).
- [80] H. Zhao, M. S. Rudner, R. Moessner, and J. Knolle, Anomalous random multipolar driven insulators, *Phys. Rev. B* **105**, 245119 (2022).
- [81] P. Das, D. Singh Bhakuni, L. F. Santos, and A. Sharma, Periodically and quasiperiodically driven-anisotropic dicke model, arXiv e-prints, arXiv (2023).
- [82] B. Mukherjee, A. Sen, D. Sen, and K. Sengupta, Restoring coherence via aperiodic drives in a many-body quantum system, *Phys. Rev. B* **102**, 014301 (2020).
- [83] H. Zhao, F. Mintert, and J. Knolle, Floquet time spirals and stable discrete-time quasicrystals in quasiperiodically driven quantum many-body systems, *Phys. Rev. B* **100**, 134302 (2019).
- [84] P. T. Dumitrescu, J. G. Bohnet, J. P. Gaebler, A. Hankin, D. Hayes, A. Kumar, B. Neyenhuis, R. Vasseur, and A. C. Potter, Dynamical topological phase realized in a trapped-ion quantum simulator, *Nature* **607**, 463 (2022).
- [85] P. W. Anderson, Absence of diffusion in certain random lattices, *Phys. Rev.* **109**, 1492 (1958).
- [86] K. Agarwal, S. Gopalakrishnan, M. Knap, M. Müller, and E. Demler, Anomalous diffusion and griffiths effects near the many-body localization transition, *Phys. Rev. Lett.* **114**, 160401 (2015).
- [87] D. F. Martinez and R. A. Molina, Delocalization induced by low-frequency driving in disordered tight-binding lattices, *Phys. Rev. B* **73**, 073104 (2006).
- [88] E. Abrahams, P. W. Anderson, D. C. Licciardello, and T. V. Ramakrishnan, Scaling theory of localization: Absence of quantum diffusion in two dimensions, *Phys. Rev. Lett.* **42**, 673 (1979).
- [89] D. M. Basko, I. L. Aleiner, and B. L. Altshuler, Metal-insulator transition in a weakly interacting many-electron system with localized single-particle states, *Annals of physics* **321**, 1126 (2006).
- [90] M. Žnidarič, T. Prosen, and P. Prelovšek, Many-body localization in the Heisenberg XXZ magnet in a random field, *Phys. Rev. B* **77**, 064426 (2008).
- [91] D. J. Luitz, N. Laflorencie, and F. Alet, Many-body localization edge in the random-field heisenberg chain, *Phys. Rev. B* **91**, 081103 (2015).
- [92] A. Pal and D. A. Huse, Many-body localization phase transition, *Phys. Rev. B* **82**, 174411 (2010).
- [93] J. Šuntajs, J. Bonča, T. Prosen, and L. Vidmar, Quantum chaos challenges many-body localization, *Phys. Rev. E* **102**, 062144 (2020).
- [94] D. Abanin, J. Bardarson, G. De Tomasi, S. Gopalakrishnan, V. Khemani, S. Parameswaran, F. Pollmann, A. Potter, M. Serbyn, and R. Vasseur, Distinguishing localization from chaos: Challenges in finite-size systems, *Annals of Physics* **427**, 168415 (2021).
- [95] T. Hartmann, F. Keck, H. J. Korsch, and S. Mossmann, Dynamics of Bloch oscillations, *New Journal of Physics* **6**, 2 (2004).
- [96] B. C. Hall, *Lie Groups, Lie Algebras, and Representations*, Vol. 222 (Springer International Publishing, 2015).

- [97] See supplementary for details of calculations, additional data, and finite-size effects, .
- [98] M. A. Nielsen and I. L. Chuang, *Quantum Computation and Quantum Information: 10th Anniversary Edition* (Cambridge University Press, 2010).
- [99] I. Peschel, Calculation of reduced density matrices from correlation functions, *Journal of Physics A: Mathematical and General* **36**, L205 (2003).
- [100] N. Roy and A. Sharma, Entanglement contour perspective for “strong area-law violation” in a disordered long-range hopping model, *Phys. Rev. B* **97**, 125116 (2018).
- [101] *Since the frequency of the drive considered is small, the data corresponding to DL and ADL seem to overlap; however, we have checked that for higher frequencies, while a slow relaxation is generic, tuning at DL results in a further slowing down of the dynamics .*
- [102] D. W. Hone and M. Holthaus, Locally disordered lattices in strong ac electric fields, *Phys. Rev. B* **48**, 15123 (1993).
- [103] D. N. Page, Average entropy of a subsystem, *Phys. Rev. Lett.* **71**, 1291 (1993).
- [104] Y. Bar Lev, G. Cohen, and D. R. Reichman, Absence of diffusion in an interacting system of spinless fermions on a one-dimensional disordered lattice, *Phys. Rev. Lett.* **114**, 100601 (2015).
- [105] D. J. Luitz and Y. B. Lev, The ergodic side of the many-body localization transition, *Annalen der Physik* **529**, 1600350 (2017).
- [106] T. L. M. Lezama, S. Bera, and J. H. Bardarson, Apparent slow dynamics in the ergodic phase of a driven many-body localized system without extensive conserved quantities, *Phys. Rev. B* **99**, 161106 (2019).
- [107] D. S. Bhakuni, L. F. Santos, and Y. B. Lev, Suppression of heating by long-range interactions in periodically driven spin chains, *Phys. Rev. B* **104**, L140301 (2021).
- [108] D. S. Bhakuni, S. Dattagupta, and A. Sharma, Effect of noise on Bloch oscillations and Wannier-Stark localization, *Phys. Rev. B* **99**, 155149 (2019).
- [109] P. Weinberg and M. Bukov, QuSpin: a Python package for dynamics and exact diagonalisation of quantum many body systems part I: spin chains, *SciPost Phys.* **2**, 003 (2017).
- [110] P. Weinberg and M. Bukov, QuSpin: a Python package for dynamics and exact diagonalisation of quantum many body systems. Part II: bosons, fermions and higher spins, *SciPost Phys.* **7**, 020 (2019).

# Supplementary material: Dynamical localization and slow dynamics in quasiperiodically-driven quantum systems

Vatsana Tiwari,<sup>1</sup> Devendra Singh Bhakuni,<sup>2</sup> and Auditya Sharma<sup>1,\*</sup>

<sup>1</sup>*Department of Physics, Indian Institute of Science Education and Research, Bhopal 462066, India*

<sup>2</sup>*Department of Physics, Ben-Gurion University of the Negev, Beer-Sheva 84105, Israel*

## I. FIBONACCI DRIVING

### A. Non-interacting Limit

For the Fibonacci sequence, we define the unitary operators  $U_0 = e^{-iTH_A}$ , and  $U_1 = e^{-iTH_B}$  corresponding to the electric field  $\pm F$  respectively and generate the subsequent evolution according to the Fibonacci sequence [1]:

$$U_n = U_{n-2}U_{n-1}, \quad n \geq 2. \quad (1)$$

Fig. 1(a) shows the Fourier spectrum of the Fibonacci sequence defined as

$$\Gamma_k = \frac{1}{N} \sum_{j=1}^N \tau_j \exp\left(\frac{i2\pi k(j-1)}{N}\right), \quad (2)$$

where we calculate the Fourier spectrum using the first  $N$  terms of the sequence  $\{\tau_j\}$ , and  $k = 0, 1, 2, \dots, N-1$ .

For simplicity, let us first study the stroboscopic unitary operator defined at Fibonacci level  $m = 2$  with two pulses  $A$  and  $B$  as

$$U(N=2) = U_B U_A = \exp(-iTH_B) \exp(-iTH_A). \quad (3)$$

Using the BCH formula [2]:

$$e^X e^Y = \exp\left[X + Y + \frac{1}{2}[X, Y] + f([X, Y, \dots]) + \dots\right], \quad (4)$$

we get

$$U(N=2) = U_B U_A \equiv \exp(-2iTH_{BA}^{\text{eff}}), \quad (5)$$

where

$$H_{BA}^{\text{eff}} = \Delta_f \left[ \hat{K} e^{-i\frac{FT}{2}} + \hat{K}^\dagger e^{i\frac{FT}{2}} \right]. \quad (6)$$

Here,  $\Delta_f = \frac{-\Delta}{4} \frac{\sin(FT/2)}{(FT/2)}$ ,  $T = \frac{2\pi}{\omega}$ . Thus, we observe from Eq.(6) that the coefficients of  $\hat{K}$  and  $\hat{K}^\dagger$  get renormalized. By tuning the amplitude of the drive at  $F/\omega = n$  ( $n \in \mathbb{Z}$ ), the effective hopping term vanishes, and

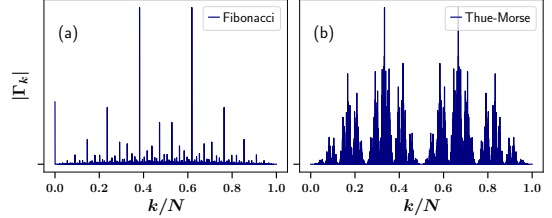


Figure 1. Fourier spectrum of (a) Fibonacci-sequence, and (b) Thue-Morse sequence.

$U(N=2)$  (Eq. (3)) takes the form of an identity operator which implies that any state will return to its initial position after this time period and hence will be dynamically localized. Next, let us consider the case of  $m = 4$ , where we have 5 pulses:  $A, B, A, A, B$ . We can define the stroboscopic unitary operator as a product of the operators  $U_A$  and  $U_B$ :

$$U(N=5) = U_B U_A U_A U_B U_A. \quad (7)$$

It is useful to pair up consecutive unitary operators associated with different types of pulses ( $A$  and  $B$ ); we thus define the Floquet unitary operators  $U_C$  and  $U_{C'}$ :

$$U_C = U_B U_A \equiv \exp(-2iTH_{BA}^{\text{eff}}), \quad (8)$$

$$H_{BA}^{\text{eff}} = \Delta_f \left[ \hat{K} e^{-i\frac{FT}{2}} + \hat{K}^\dagger e^{i\frac{FT}{2}} \right], \quad (9)$$

$$U_{C'} = U_A U_B \equiv \exp(-2iTH_{AB}^{\text{eff}}), \quad (10)$$

$$H_{AB}^{\text{eff}} = \Delta_f \left[ \hat{K} e^{i\frac{FT}{2}} + \hat{K}^\dagger e^{-i\frac{FT}{2}} \right]. \quad (11)$$

Using Eq. (8), and (10), we can rewrite Eq. (7) as:

$$\begin{aligned} U(N=5) &= U_C U_{C'} U_A, \\ &\equiv \exp(-2iTH_{BA}^{\text{eff}}) \exp(-2iTH_{AB}^{\text{eff}}) U_A. \end{aligned} \quad (12)$$

It is clear from Eq. (9) and Eq. (11) that at  $F = n\omega$ , both  $U_C$  and  $U_{C'}$  become the identity operator and the effective dynamics at Fibonacci level  $m = 4$  is governed by  $U_A$ :

$$U(N=5) \equiv U_A = \exp(-iTH_A). \quad (13)$$

A careful analysis of the Fibonacci sequence at higher levels suggests that the product of two different consecutive unitary operators ( $U_A$  and  $U_B$ ) yields an identity

\* [auditya@iiserb.ac.in](mailto:auditya@iiserb.ac.in)



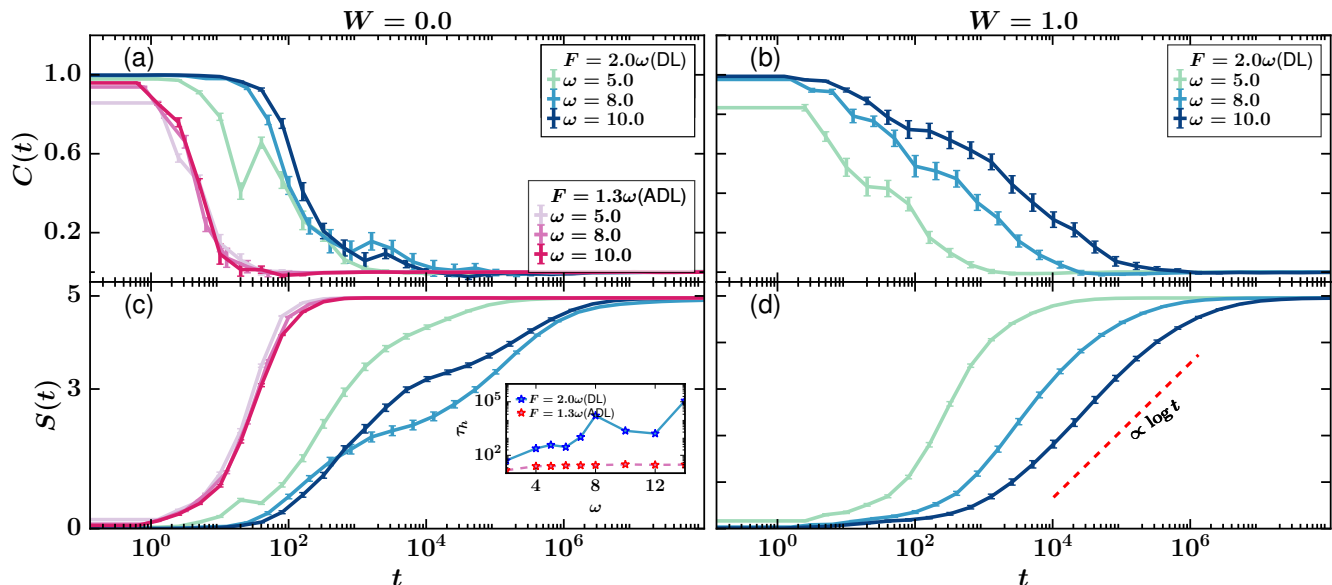


Figure 4. (a,c): Auto-correlation  $C(t)$  and half chain entanglement entropy  $S(t)$  for Thue-Morse driven clean ( $W = 0.0$ ) interacting system. In (a) and (c), the plots in pink shades correspond to the parameters being tuned away from dynamical localization (DL) ( $F = 2.0\omega$ ), and blue shade plots correspond to the parameters being tuned at dynamical localization (DL) ( $F = 1.3\omega$ ), and blue shade plots correspond to the parameters being tuned at dynamical localization (DL) ( $F = 2.0\omega$ ). Inset(c): Heating time  $\tau_h$  vs frequency  $\omega$ . (b, e):  $C(t)$  and  $S(t)$  for Thue-Morse driven disordered ( $W = 1.0$ ) interacting system. We have averaged over 100 disorder realizations. In (d), the red dashed line is drawn to show logarithmic growth of entanglement entropy ( $S(t) \propto \log t$ ) for  $\omega = 10$ . The other system parameters are  $\Delta = 4.0, U = 1.0, F = 2.0\omega$ , and system size  $L = 16$ .

where we start with the unitary operators  $U_1 = U_B U_A$ ,  $\tilde{U}_1 = U_A U_B$  with  $U_A = e^{-iTH_A}$  and  $U_B = e^{-iTH_B}$ . Fig. (1)(b) shows the Fourier spectrum of the Thue-Morse sequence.

To study the dynamics of Thue-Morse driven systems, we evaluate the Floquet unitary operator stroboscopically. Let us first compute the time evolution operator at Thue-Morse level  $m = 2$ , where the drive comes with  $4(= 2^2)$  pulses:  $A, B, B, A$ . Hence, we can write the time evolution operator stroboscopically as:

$$U(N = 4) = U_A U_B U_B U_A. \quad (16)$$

From the recurrence relation (15), we see that the Thue-Morse sequence always yields pairs of  $U_A$  and  $U_B$ , with the total number of these operators being an exact power of 2. Hence, we can evaluate Eq.(16) as

$$U(N = 4) = U_{C'} U_C, \quad (17)$$

where the operators  $U_C$  and  $U_{C'}$  are as defined earlier:

$$U_C = U_B U_A \equiv \exp(-2iTH_{BA}^{\text{eff}}), \quad (18)$$

$$H_{BA}^{\text{eff}} = \Delta_f \left[ \hat{K} e^{-i\frac{FT}{2}} + \hat{K}^\dagger e^{i\frac{FT}{2}} \right], \quad (19)$$

$$U_{C'} = U_A U_B \equiv \exp(-2iTH_{AB}^{\text{eff}}), \quad (20)$$

$$H_{AB}^{\text{eff}} = \Delta_f \left[ \hat{K} e^{i\frac{FT}{2}} + \hat{K}^\dagger e^{-i\frac{FT}{2}} \right]. \quad (21)$$

Using the BCH formula(4), we can rewrite Eq. (17) in

terms of an effective Hamiltonian as

$$U(N = 2^2) \equiv \exp(-2^2 iTH_{\text{eff}}), \quad (22)$$

where

$$H_{\text{eff}} = \Delta_{\text{eff}} \left( \hat{K} + \hat{K}^\dagger \right), \quad \Delta_{\text{eff}} = \frac{-\Delta \sin FT}{4 FT}. \quad (23)$$

Here,  $\Delta_{\text{eff}}$  is the effective hopping strength which vanishes when the drive strength  $F$  is tuned to be a half integer multiple of drive frequency  $\omega$  i.e.  $F/\omega = n/2, n \in \mathbb{Z}$ . At these specific values, Thue-Morse driving causes the dynamical localization of the non-interacting system.

Following the recurrence relation defined in Eq. (15), we can construct the time evolution operator  $U(N = 2^m)$  for higher Thue-Morse level  $m$  having  $2^m$  pulses, which is the product of a string of Floquet unitary operators  $U_A$  and  $U_B$ . We observe that the full product of unitary operators at each Thue-Morse level  $m > 2$  may be constructed in terms of groups of four operators of two types: ' $U_A U_B U_B U_A$ ' and ' $U_B U_A U_A U_B$ '. Since  $U_{C'} U_C \equiv U_C U_{C'}$  (from Eq. (18)-(20)), following the steps from Eq. (16)-Eq. (22), we can again get a generalized form of the unitary operator  $U(N = 2^m)$ :

$$U(N = 2^m) \equiv \left( \exp(-2^2 iTH_{\text{eff}}) \right)^{2^{m-2}} \\ U(N = 2^m) \equiv \exp(-2^m iTH_{\text{eff}}). \quad (24)$$

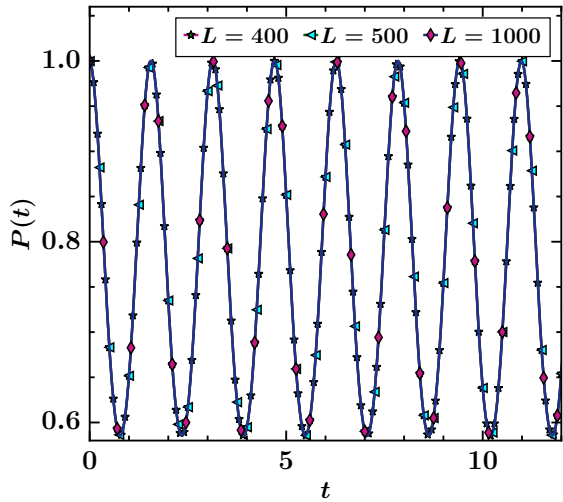


Figure 5. Dynamics of return probability  $P(t)$  at dynamical localization point ( $F = 2\omega$ ) for Thue-Morse driven clean ( $W = 0$ ) non-interacting system for system sizes  $L = 400, 500, 1000$ . The other parameters are  $\Delta = 4.0, \omega = 2.0, F = 2.0, U = 0.0$ .

Hence, we observe that the dynamics of the Thue-Morse driven system is governed by  $H_{\text{eff}}$  which is simply a nearest-neighbor tight-binding Hamiltonian with renormalized hopping strength  $\Delta_{\text{eff}}$  (Eq. (23)). In the main Letter, we show numerical evidence for this analytical result in the form of return probability  $P(t)$  and entanglement entropy  $S(t)$ . Next, we include disorder in addition to the Thue-Morse drive. The disorder destroys the dynamical localization and we observe a sub-linear growth of entanglement entropy,  $S(t) \propto t^\gamma, \gamma < 1$  as shown in the main Letter (Fig.(1) of the main Letter).

Finally, we comment on the possibility of dynamical localization for any sequence of random unitary operators [3]. While the system is delocalized when the electric field is randomly flipped at arbitrary times (white-noise) [4], dynamical localization can be engineered for any random sequence of unitary operators applied for an equal amount of time and with proper tuning of the parameters. This can be accomplished by a method similar to the above where a proper choice of the parameters can yield an effective unitary operator that is equal to the identity operator.

### B. Interacting Limit

We study the behavior of the auto-correlation function  $C(t) = 4\langle \hat{S}_{L/2}^z(t)\hat{S}_{L/2}^z(0) \rangle$  and growth of entanglement entropy  $S(t)$  for the Thue-Morse driven clean (Fig. 4(a,c)) and disordered interacting (Fig. 4(b,d)) system. For the clean system, the dynamics for  $F/\omega = 1.3$  (away from dynamical localization) quickly approaches the Page value (pink shade curves), whereas for  $F/\omega =$

2.0, the system relaxes to the infinite temperature state very slowly (blue shade curves). To distinguish the dynamics of the system at the dynamical localization (DL) point and away from the dynamical localization (ADL) point, we plot the heating time as a function of frequency ( $\tau_h$  vs  $\omega$ ) in the inset of Fig.4(c) for  $F = 2.0\omega$  (DL), and  $F = 1.3\omega$  (ADL). It clearly shows that the significant suppression of hopping strength at DL leads to a slow heating of the system. In contrast, the system quickly reaches a featureless infinite temperature state on tuning the parameters away from DL.

In Fig. 4(b,d), we focus on the ergodic side of the disordered system by fixing the disorder strength to be  $W = 1.0$ , and drive the system at the dynamical localization point  $F/\omega = 2.0$ .  $C(t)$  and  $S(t)$  exhibit the same behavior as shown in the Fibonacci driven case in the main Letter. The entanglement entropy attains the Page value,  $S_{\text{Page}} = \frac{1}{2}(L \ln 2 - 1)$  (corresponding to the infinite temperature state) [5] logarithmically slowly ( $S(t) \propto \log t$ ) (Fig. 4(d)).

### III. FINITE-SIZE EFFECTS

To show the system size independence of our chief findings for driven non-interacting and interacting systems, we show the data for different system sizes in Fig. 5, 6 and Fig. 7. In the non-interacting clean limit, we study return probability  $P(t)$  at the dynamical localization point for different system sizes  $L = 400, 500, 1000$  in Fig. 5, and find that the dynamics of return probability remains consistent for all the considered system sizes. For the non-interacting disordered system, we study the return probability  $P(t)$ , and half chain entanglement entropy  $S(t)$  for various system sizes  $L = 100, 200, 400, 600$ . In Fig. 6(a) and Fig. 6(b), the return probability  $P(t)$  and half chain entanglement entropy  $S(t)$  exhibit slow relaxation for all the studied system sizes. For the interacting model, we study auto-correlation function  $C(t)$ , and half chain entanglement entropy  $S(t)$  for system sizes  $L = 10, 12, 14$  and show the data for clean and disordered cases in Fig.(7(a,c)) and Fig.(7(b,d)). In both the cases, we observe that the dynamics of entanglement entropy for small system sizes exhibits slow relaxation to the Page value  $S_{\text{Page}} = \frac{1}{2}(L \ln 2 - 1)$  corresponding to an infinite-temperature state, and hence is in complete agreement with the findings for system size  $L = 16$  (as shown in the main Letter). The dynamics of autocorrelation function  $C(t)$  also exhibits slow relaxation for all the studied system sizes. Thus, we can conclude that the quasiperiodic drive induces slow relaxation in the non-interacting and interacting disordered system. While  $S(t)$  follows sub-linear growth ( $S(t) \propto t^\gamma, \gamma < 1$ ) in the non-interacting case, we observe logarithmic growth of entanglement entropy,  $S(t) \propto \log t$  in the interacting case. We have also checked the results for the Thue-Morse driven system and confirm that this too yields similar behavior.

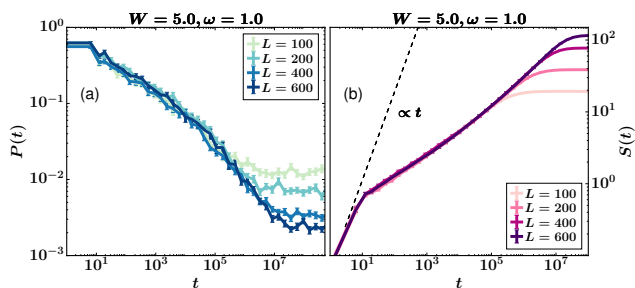


Figure 6. (a) Dynamics of return probability  $P(t)$  and (b) Half chain entanglement entropy  $S(t)$  for Fibonacci driven disordered ( $W = 5.0$ ) non-interacting system for system sizes  $L = 100, 200, 400, 600$ . The black dashed line indicates the linear growth of entanglement entropy ( $S(t) \propto t$ ). The other parameters are  $\Delta = 4.0, \omega = 1.0, F = 2.0, U = 0.0$ .

#### IV. PERIODICALLY DRIVEN MODEL

##### A. Non-interacting Limit

To understand the dynamics of quasiperiodically driven systems, we start with the analysis of a periodically driven system defined by the Hamiltonian

$$H(t) = \begin{cases} H_A = D + D_0 + E, & 0 \leq t \leq T/2 \\ H_B = D + D_0 - E, & T/2 < t \leq T, \end{cases} \quad (25)$$

where,

$$\begin{aligned} D &= -\frac{\Delta}{4} \sum_{j=0}^{L-2} (c_j^\dagger c_{j+1} + h.c.) = -\frac{\Delta}{4} (\hat{K} + \hat{K}^\dagger), \\ D_0 &= \sum_{j=0}^{L-1} h_j \left( n_j - \frac{1}{2} \right), \\ E &= F \sum_{j=0}^{L-1} j \left( n_j - \frac{1}{2} \right) = F \hat{N}. \end{aligned} \quad (26)$$

Now, we define the time evolution operator  $U = U_A U_B$  and extract the effective Hamiltonian  $H_{\text{eff}}$ :

$$U = U_A U_B = \exp(-i\frac{T}{2} H_A) \exp(-i\frac{T}{2} H_B) \equiv \exp(-i T H_{\text{eff}}) \quad (27)$$

where  $H_{\text{eff}}$  is defined as

$$\begin{aligned} H_{\text{eff}} &= \frac{-1}{iT} \log \left[ \exp(-i\frac{T}{2} H_A) \exp(-i\frac{T}{2} H_B) \right], \\ &= H_\Delta + D_0 + H_{LRH}. \end{aligned}$$

Using the BCH expansion [2] we can work out

$$H_\Delta = \Delta_{\text{eff}} \{ \hat{K} e^{-iFT/4} + \hat{K}^\dagger e^{iFT/4} \}, \quad (28)$$

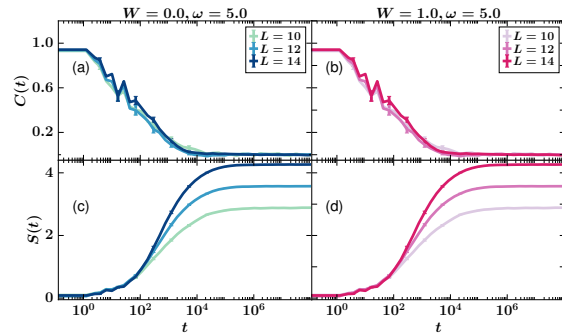


Figure 7. Comparison of dynamics of Fibonacci driven clean ( $W = 0.0$ ) and disordered ( $W = 1.0$ ) interacting system. (a,b): Auto-correlation function  $C(t)$  at driving frequency  $\omega = 5.0$  for different system sizes  $L = 10, 12, 14$ . (c,d): Half chain entanglement entropy  $S(t)$  at driving frequency  $\omega = 5.0$  for different system sizes  $L = 10, 12, 14$ . The other parameters are  $\Delta = 4.0, F = 2\omega, U = 1.0$ .

with  $\Delta_{\text{eff}} = \frac{-\Delta/4}{F\pi/2\omega} \sin(F\pi/2\omega)$  as before.  $H_{LRH}$  contains the longer-range hopping terms and for which we obtain an approximate expression (by considering upto 5th order terms in the BCH expansion):

$$\begin{aligned} H_{LRH} &= \frac{-\Delta}{4} FT \sum_j \left[ d_j (a + ib) (c_{j+2}^\dagger c_j + h.c.) \right. \\ &\quad + \{ (q_1 b_j^2 + q_2 b_j) + i(p_1 b_j^2 + p_2 b_j) \} \\ &\quad \left. (c_{j+1}^\dagger c_j + h.c.) + b_j (c_{j+1}^\dagger c_{j+1} - c_j^\dagger c_j) \right], \end{aligned} \quad (29)$$

where  $d_j = b_{j+1} - b_j, b_j = h_{j+1} - h_j$ , and  $a = \frac{-13T^3(\Delta F)}{11520}, b = \frac{-\Delta T^2}{384}, q_1 = \frac{-7FT^3}{1440}, p_1 = \frac{-T^2}{48}, q_2 = \frac{-F^2 T^3}{480}, p_2 = \frac{-T^2 F}{96} (F - 1)$ .

##### 1. High-frequency Driving

If driving frequency  $\omega$  is larger than the local bandwidth  $\Delta_\xi$  of a system of size of the order of the localization length  $\xi$  (it implies that  $\omega \gg \Delta, W$ ), we can ignore the terms with higher power of  $T (= 2\pi/\omega)$ . Hence, we recover an effective Hamiltonian  $H_{\text{eff}}$ :

$$H_{\text{eff}} = H_\Delta + D_0. \quad (30)$$

At dynamical localization point,  $F = 2n\omega$ ,  $\Delta_{\text{eff}} = \frac{-\Delta/4}{F\pi/2\omega} \sin(F\pi/2\omega) \rightarrow 0$ , and we get hopping suppression from  $\Delta$  to  $\Delta_{\text{eff}}$ . It leads to an increased normalized disorder strength from  $W/\Delta$  to  $W/\Delta_{\text{eff}}$ . Thus, the periodically driven model shows the persistence of *Anderson localization* when the drive-parameters are tuned at the dynamical localization (DL) point at high frequency [6, 7].

Away from dynamical localization (ADL), if we again analyse  $\Delta_{\text{eff}}$  at high frequency:

$$\begin{aligned}\Delta_{\text{eff}} &= \frac{-\Delta/4}{F\pi/2\omega} \sin(F\pi/2\omega) \equiv \frac{\Delta}{4}; \quad (\Delta/\omega \ll 1), \\ H_{\text{eff}} &= \frac{-\Delta}{4} \left( \hat{K} e^{-iFT/4} + \hat{K}^\dagger e^{iFT/4} \right) + D_0.\end{aligned}\quad (31)$$

Hence, we recover an Anderson-like model Hamiltonian at high frequency driving even at points away from DL. Therefore, we observe that high-frequency periodic driving preserves Anderson localization even away from DL.

## 2. Low Frequency Driving

However, at low-frequency when driving frequency  $\omega$  is smaller than the local bandwidth  $\Delta_\xi$  (i.e.  $\omega \ll \Delta, W$ ),  $H_{LRH}$  (Eq.(29)) which contains the higher order hopping terms of the effective Hamiltonian plays an important role. This causes delocalization at DL as well as away from DL.

## B. Interacting Limit

The Hamiltonian here is:

$$\begin{aligned}H(t) &= \begin{cases} H_A = D + D_0 + V + E, & 0 \leq t \leq T/2 \\ H_B = D + D_0 + V - E, & T/2 < t \leq T, \end{cases} \\ V &= \sum_{j=0}^{L-2} U(n_j - \frac{1}{2})(n_{j+1} - \frac{1}{2}).\end{aligned}$$

Following the analysis of the non-interacting disordered Floquet Hamiltonian, we can again write an effective Hamiltonian :

$$H_{\text{eff}} = H_\Delta + D_0 + V + H_{LR}, \quad (32)$$

where

$$H_{LR} = H_{LRH} + H_{\text{int}}(V, D, D_0, E), \quad (33)$$

and

$$\begin{aligned}H_{\text{int}}(V, D, D_0, E) &= -\frac{(-iT)^2}{12} \{ [V, [H_A, [E, D]]] \\ &\quad + [H_B, A] + [D + D_0 + V, A] \} + \dots,\end{aligned}\quad (34)$$

where  $A = [V, [E, D]]$ . For the case of the interacting Hamiltonian, we obtain  $H_{LR}$  by replacing  $D_0$  with  $D_0 + V$  in the computation of the non-interacting limit. Again it is worth noting that  $H_{LR}$  comes with higher powers of  $T$ .

### 1. High-frequency Driving

Similar to the non-interacting limit, we can ignore  $H_{LR}$  at high-frequency  $\omega (\gg \Delta)$ , and get an effective Hamiltonian as the sum of  $H_\Delta, D_0$ , and  $V$ :

$$H_{\text{eff}} = H_\Delta + D_0 + V, \quad (35)$$

which is in the form of a *standard MBL model*, with hopping strength  $\Delta_{\text{eff}}$ .

At DL,  $\Delta_{\text{eff}} = \frac{-\Delta/4}{F\pi/2\omega} \sin(F\pi/2\omega) \rightarrow 0$ , and normalized disorder increases from  $\frac{W}{\Delta}$  to  $\frac{W}{\Delta_{\text{eff}}}$ , hence leads to *drive-induced MBL* [8]. At this frequency, the system is endowed with a set of local integrals of motion which freeze transport and localize excitations. It is worth noting that  $\omega_c$ , the threshold value above which localization occurs, varies with  $W$ .

ADL, from a series expansion of  $\sin c$  function:

$$\Delta_{\text{eff}} = \frac{-\Delta/4}{F\pi/2\omega} \sin(F\pi/2\omega) \equiv \frac{\Delta}{4}. \quad (36)$$

Hence,

$$H_{\text{eff}} = \frac{-\Delta}{4} \{ \hat{K} e^{-iFT/4} + \hat{K}^\dagger e^{iFT/4} \} + D_0 + V. \quad (37)$$

Eq.(37) is again an *MBL-like* Hamiltonian.

- 
- [1] S. Maity, U. Bhattacharya, A. Dutta, and D. Sen, Fibonacci steady states in a driven integrable quantum system, *Phys. Rev. B* **99**, 020306 (2019).
- [2] B. C. Hall, *Lie Groups, Lie Algebras, and Representations*, Vol. 222 (Springer International Publishing, 2015).
- [3] H. Zhao, F. Mintert, R. Moessner, and J. Knolle, Random multipolar driving: Tunably slow heating through spectral engineering, *Phys. Rev. Lett.* **126**, 040601 (2021).
- [4] V. Tiwari, D. S. Bhakuni, and A. Sharma, Noise-induced dynamical localization and delocalization, *Phys. Rev. B* **105**, 165114 (2022).
- [5] D. N. Page, Average entropy of a subsystem, *Phys. Rev. Lett.* **71**, 1291 (1993).
- [6] D. W. Hone and M. Holthaus, Locally disordered lattices in strong ac electric fields, *Phys. Rev. B* **48**, 15123 (1993).
- [7] D. F. Martinez and R. A. Molina, Delocalization induced by low-frequency driving in disordered tight-binding lattices, *Phys. Rev. B* **73**, 073104 (2006).
- [8] E. Bairey, G. Refael, and N. H. Lindner, Driving induced many-body localization, *Phys. Rev. B* **96**, 020201 (2017).